A Single Transition State Serves Two Mechanisms. The Branching Ratio for $CH_2O^{\bullet-}$ + CH_3Cl on Improved Potential Energy Surfaces

Jie Li,[†] Sason Shaik,[‡] and H. Bernhard Schlegel*,[†]

Department of Chemistry, Wayne State University, Detroit, Michigan 48202, and Department of Organic Chemistry and the Lise Meitner-Minerva Center of Computational Chemistry, Hebrew University, Jerusalem 91904, Israel

Received: November 2, 2005; In Final Form: January 12, 2006

The reaction of formaldehyde radical anion with methyl chloride, $CH_2O^{\bullet-} + CH_3Cl$, is an example in which a single transition state leads to two products: substitution at carbon (Sub(C), $CH_3CH_2O^{\bullet} + Cl^-$) and electron transfer (ET, $CH_2O + CH_3^{\bullet} + Cl^-$). The branching ratio for this reaction has been studied by ab initio molecular dynamics (AIMD). The energies of transition states and intermediates were computed at a variety of levels of theory and compared to accurate energetics calculated by the G3 and CBS-QB3 methods. A bond additivity correction has been constructed to improve the Hartree−Fock potential energy surface (BAC-UHF). A satisfactory balance between good energetics and affordable AIMD calculations can be achieved with BH&HLYP/6-31G(d) and BAC-UHF/6-31G(d) calculations. Approximately 200 ab initio classical trajectories were calculated for each level of theory with initial conditions sampled from a thermal distribution at 298 K at the transition state. Three types of trajectories were distinguished: trajectories that go directly to ET product, trajectories that go to Sub(C) product, and trajectories that initially go into the Sub(C) valley and then dissociate to ET products. The BH&HLYP/6-31G(d) calculations overestimate the number of nonreactive and direct ET trajectories because the transition state is too early. For the BH&HLYP and BAC-UHF methods, about one-third of the trajectories that initially go into the Sub(C) valley dissociate to ET products, compared to just over half with UHF/6-31G(d) in the earlier study. This difference can be attributed to a better value for the calculated energy release from the initial transition state and to an improved Sub(C) → ET barrier height with the BH&HLYP and BAC-UHF methods.

Introduction

Borderline reactions occur when two related mechanisms start to merge and generate a mechanism with combined properties.[1,2] The entanglement of the mechanisms and their crossover in a borderline reaction is an intriguing topic that has attracted much attention recently. In the borderline region, the reaction can occur through two different transition states with similar reaction rates, or more interestingly, the reaction can proceed via one single transition state to two different products. A well-known example of the latter case is the reaction between ketyl radical anions and alkyl halides in which both electron transfer (ET) products and substitution at carbon (Sub(C)) products can be formed via the same, tightly bound transition state.[3−14] Such cases are especially attractive, since a slight change of the potential energy surface around the transition state may vary the branching ratio of the products.

The relationship between electron transfer and substitution mechanisms in this system has been the subject of numerous theoretical and experimental studies.[3−14] Electron transfer can occur through two pathways. In one case, an electron can be transferred via an outer sphere species which involves a weak interaction and surface hopping. In the other case, the reaction can proceed via a tightly bound transition state, which may also lead to substitution products.[3,4,7−15] Early mechanistic studies were carried out by Garst on the reactions of benzophenone ketyls with alkyl bromides,[16,17] where it was shown that, along with an ET mechanism that leads to radical formation, one also obtains alkylation products. More recent mechanistic studies were carried out by Screttas and Michascrettas,[18] who used ^{13}C spin transfer NMR techniques to try to quantify the inner sphere tightly bound transition states. These reactions and analogous ones have been considered to have the borderline character between ET and Sub(C) mechanisms,[19] since the observed rate constants were 2−3 orders of magnitude larger than those expected for ET reactions in the outer sphere mechanism. In some of the reactions,[19−21] tightly bonded transition states were suggested because the entropy of activation was found to be quite negative (−5 to −16 eu). Similar conclusions were drawn by Eberson.[22] As such, these processes may fall into the category of the present model where a single transition state serves two mechanisms. Using the usual tools of physical organic chemistry, it may be difficult to distinguish these intriguing situations from the more pedestrian case characterized by two separate transition states. Computational methods, particularly the simulation of molecular dynamics by ab initio classical trajectory calculation can provide valuable insights into these novel reactions that are unavailable through experimental methods.

Reactions between ketyl radical anions and alkyl halides that exhibit the richness of borderline mechanisms have been studied by both reaction path following and ab initio trajectory calculations.[3,4,7−15] As seen in Scheme 1, after the transition state, the potential energy surface bifurcates into two valleys: the ET product valley and the Sub(C) product valley. Of these reactions, the $CH_2O^{\bullet-} + CH_3Cl$ system has been the most

* Corresponding author. E-mail: hbs@chem.wayne.edu.
[†] Wayne State University.
[‡] Hebrew University.

10.1021/jp0563336 CCC: $33.50
Published on Web 02/04/2006

SCHEME 1

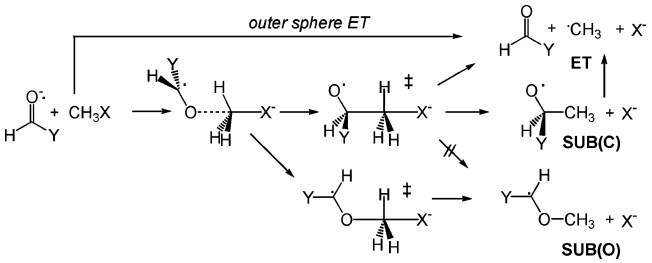

intensively studied.[3,4,7−15] The tightly bound transition state has been well characterized at a variety of levels of theory in previous work.[3,4,7−15] Reaction path following showed that the steepest descent path using *Z*-matrix internal coordinates results in ET products, while the reaction path using mass-weighted coordinates (intrinsic reaction coordinate, IRC) leads to a ridge. With unrestricted Hartree−Fock (UHF) calculations, the reaction path proceeds to the Sub(C) valley, but with restricted open shell Hartree−Fock (ROHF) calculations, the path falls back into the ET valley.[11] The effect of substituents on the direction of the reaction has been studied by Yamataka, Aida, and Dupuis (YAD) and by our group. From a series of ab initio classical trajectory calculations on $CH_2O^{\bullet-} + CH_3X$ (X = F, Cl, Br),[11] $NCCHO^{\bullet-} + CH_3Cl$,[11,14] and $NCCHO^{\bullet-} + (CH_3)_2CHCl$,[14] it was found that shorter C−C distances in the transition states and weaker electron donors favor Sub(C) over ET; cyano substitution favored the substitution reaction and bulky substitution favored electron transfer. A closer look at the molecular dynamics simulations revealed three types of trajectories:[12−15] simple ones that go directly to Sub(C) products or directly to ET products and more complex ones that go first to the Sub(C) valley and then finally dissociate to ET products. Trajectories leading to the Sub(C) valley produced $CH_3CH_2O^{\bullet}$ fragments with considerable internal energy, and some of these underwent unimolecular dissociation, yielding ET products via first-order kinetics.[15] Higher temperatures raised the amount of internal energy and increased the number of Sub(C)-to-ET trajectories.[13,15] On the other hand, solvent relaxation decreased the number of the trajectories which went from Sub(C) to ET.[13]

From the various molecular dynamics simulations, it is apparent that the branching ratio depends on the quality of the potential energy surface. The ratio of Sub(C) to direct ET trajectories depends on the position of the ridge separating the two valleys. The energy released from the transition state to Sub(C) products and the height of the barrier separating the Sub(C) and ET valleys are important factors in determining the number of the trajectories that are able to dissociate to ET products. Ab initio classical trajectory calculations with higher levels of theory are needed to clarify the dynamics of this system. Accurate gas phase energies can be calculated by compound methods such as G3 and CBS-QB3,[23−25] but these are far too costly to be used for classical trajectory calculations of the $CH_2O^{\bullet-} + CH_3Cl$ system. In the present work, we explore the effect of a number of more affordable levels of theory on the energetics and dynamics of the $CH_2O^{\bullet-} + CH_3Cl$ reaction in the gas phase. In particular, we examine the performance of various functionals for density functional theory (DFT) calculations and construct a bond additivity correction to improve the potential energy surface for molecular dynamics. In subsequent work, we will look at the effects of solvation on the energetics and dynamics.

Methods

Molecular orbital calculations were performed with the development version of the Gaussian series of programs.[26] Geometries were optimized by Hartree−Fock (HF) and density functional theory calculations. Higher accuracy energy differences were calculated by the G3[23] and CBS-QB3[24,25] methods. Molecular dynamics were studied by ab initio classical trajectory calculations using the Born−Oppenheimer approximation,[27] in which the wave function is converged at every step. The nuclei are moved by the integration of the classical equation of motion using our Hessian-based predictor-corrector algorithm.[28] For the predictor step, the equations of motion are integrated on a local quadratic surface. Then, a fifth-order polynomial is fitted to the energies, gradients, and Hessians at the beginning and end points of the predictor step. A corrector step is taken on this more accurate fitted energy surface. The Hessian is calculated analytically and followed by five updates before it is recalculated analytically again.[29]

As in our previous work,[3,15] the trajectories were started from the transition state and the initial conditions were chosen to correspond to a thermal distribution at 298 K. Motion along the transition vector was in the direction toward the products and was sampled from a thermal distribution.[30] Rotational energies were sampled from a thermal distribution of a symmetric top. For the vibrational degrees of freedom, quasiclassical normal-mode sampling was used and included both zero-point energy and thermal energy.[30,31] Trajectories were integrated with a step size of 0.5 $amu^{1/2}$ bohr. The total energy was conserved to better than 10^{-5} hartree, and total angular momentum was conserved to better than $10^{-9}\hbar$ through the use of projection. For each level of theory, approximately 200 trajectories were integrated starting from the transition state and ending with the products being well separated.

Results and Discussion

Structures and Energetics. The G3 level of theory is known to give reliable energetics (mean absolute deviation of 1.02 kcal/mol for 299 comparisons with experiment).[23] In assessing the quality of various levels of theory, the G3 method will be used as a standard. The energetics and optimized geometries for various intermediates and transition states for the $CH_2O^{\bullet-} + CH_3Cl$ reaction are shown in Figure 1. For G3 calculations, geometries are optimized by MP2(full)/6-31G(d). Earlier work showed that expanding the basis set or improving the treatment of electron correlation does not change the geometry of the initial transition state (TS) drastically.[3] The energies at a number of levels of theory are compared to the G3 calculations in Table 1. From the perspective of the dynamics of the reaction, four energy differences are particularly important: the energy release from the transition state to the Sub(C) product, to the ET product, and to the Sub(C) → ET transition state and the barrier from the Sub(C) to ET products. Previous studies showed that the chloride ion is well separated from the remaining atoms when the trajectories reach the Sub(C) and ET product valleys.[15] Hence, the relevant energy differences are the ones without the chloride bound. At the G3 level, the energy release from the TS to Sub(C), ET, and Sub(C) → ET TS are 21.2, 12.3, and 4.7 kcal/mol, respectively, and the barrier from Sub(C) to ET is 16.5 kcal/mol. The CBS-QB3 values agree very well with the G3 numbers, but neither method is practical for molecular dynamics simulations for this system.

Earlier molecular dynamics simulations were carried out at the UHF/6-31G(d) and UHF/6-31+G(d) levels of theory.[3,13−15] The energy releases from the TS to uncomplexed products are

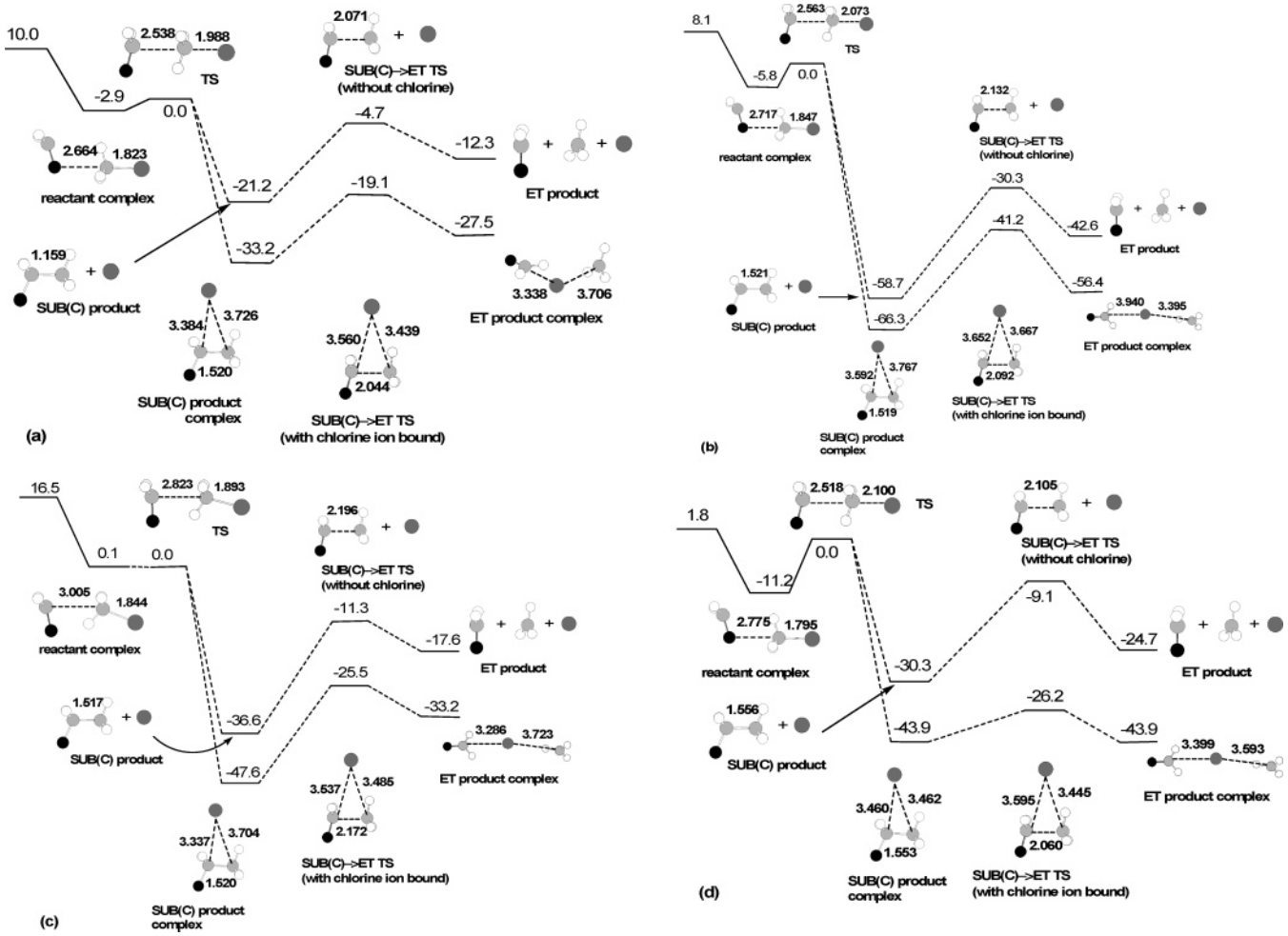

Figure 1. Optimized geometries and relative energies of the transition states and products for the Sub(C)/ET reaction: (a) G3 enthalpies and MP2/6-31G(d) geometries; (b) UHF/6-31G(d); (c) BH&HLYP/6-31G(d); (d) BAC-UHF/6-31G(d).

TABLE 1: Enthalpies of the Optimized Transition States and Products for the Sub(C)/ET Reaction[a]

	method				
structure	G3	CBS-QB3	UHF/6-31G(d)	UHF/6-31+G(d)	BAC-UHF/6-31G(d)
reactant complex	−12.9	−12.1	−13.9	−11.1	−13.0
TS	−10.0	−9.9[b]	−8.1	−1.5	−1.8
Sub(C) product complex	−43.2	−44.5	−74.4	−64.4	−45.7
ET product complex	−37.5	−36.0	−64.5	−55.8	−45.7
Sub(C) → ET TS (with chlorine ion bound)	−29.1	−29.1	−49.3	−39.7	−28.0
Sub(C) product	−31.2	−31.5	−66.8	−58.1	−32.1
ET product	−22.3	−21.5	−50.7	−43.5	−26.5
Sub(C) → ET TS (without chlorine)	−14.7	−15.5	−38.4	−30.2	−10.9

[a] Relative to the reactants, in kilocalories per mole at 298 K, 1 atm. [b] Single-point energy with the UHF optimized geometry.

too large by 25−37 kcal/mol, and the barrier from Sub(C) to ET is 12 kcal/mol too high (see Table 1). The excess energy in the Sub(C) products should lead to an elevated amount of dissociation from Sub(C) to ET for trajectories at the UHF level of theory. In hope of obtaining better agreement with the G3 calculations, we have examined density functional calculations and bond additivity corrections.

Density functional theory with its broad choice of functionals offers an alternative method for obtaining better energy differences that would more closely resemble the G3 potential energy surface. Several functionals were examined: B3LYP,[32] B3PW91,[32−36] B1LYP,[33] BH&H,[37] BH&HLYP,[37−39] MPW1PW91,[33,40] and the recently developed BMK functional.[41] Table 2 compares the energetics of these calculations to the G3 results. Functionals developed for thermochemistry, such as B3LYP, B3PW91, and B1LYP, often underestimate barrier heights by 5−10 kcal/mol.[42] More problematic is the fact that these functionals fail to give an optimized geometry for the reactant complex and the transition state for the $CH_2O^{\bullet-} + CH_3Cl$ reaction. From the reactants, the potential energy surface descends to products without a barrier. The energies for the reactant complex and the transition state reported for these functionals in Table 2 were calculated using the BH&HLYP optimized geometries. Enlarging the basis set from 6-31G(d) to CBS7 did not change the B3LYP energy releases significantly. The BH&H and BH&HLYP functionals mix in 50% of the Hartree−Fock exchange. This often improves the barriers but sometimes at the expense of the reaction energy.[42,43] As shown in Figure 1c, the TS optimized with BH&HLYP/6-31G(d) is much earlier along the reaction path than the TS optimized with MP2(full)/6-31G(d) (R_{C-C} = 2.823 vs 2.538 Å, R_{C-Cl} = 1.893 vs 1.988 Å), and the barrier from the reactant complex

TABLE 2: Enthaplies of the Optimized Transition States and Products for the Sub(C)/ET Reaction Calculated by Density Functional Methods[a]

	method							
structure	G3	B3PW91/ 6-31G(d)	B3LYP/ 6-31G(d)	B1LYP/ 6-31G(d)	BH&H/ 6-31G(d)	BH&HLYP/ 6-31G(d)	MPW1PW91/ 6-31G(d)	BMK/ 6-31G(d)
reactant complex	−12.9	−18.0[b]	12.5[b]	−18.3[b]	−20.6	−16.4	−17.0	−16.3
TS	−10.0	−19.8[b]	10.6[b]	−19.9[b]	−21.0	−16.5	−19.8[b]	−18.8[b]
Sub(C) product complex	−43.2	−62.2	−31.3	−62.4	−69.0	−64.1	−62.9	−46.9
ET product complex	−37.5	−43.1	−14.5	−47.3	−42.5	−49.7	−43.3	−30.5
Sub(C) → ET TS (with chlorine ion bound)	−29.1	−38.1	−9.2	−41.0	−41.3	−42.0	−38.8	−25.4
Sub(C) product	−31.2	−45.1	−13.7	−46.5	−51.9	−53.1	−46.5	−62.0
ET product	−22.3	−22.4	0.8	−32.0	−21.8	−34.1	−28.1	−44.8
Sub(C) → ET TS (without chlorine)	−14.7	−24.2	5.2	−26.8	−22.4	−27.8	−24.3	−39.1

[a] Relative to the reactants, in kilocalories per mole at 298 K, 1 atm. [b] Single-point energies with the BH&HLYP optimized geometry.

to the transition state is too small. The reactant complex is a little bit higher than the transition state when zero-point energy is included. The energy release from the TS to products is much better than that for Hartree−Fock with the same basis set. The MPW1PW91 and BMK functionals were developed to provide an accurate and balanced treatment for both thermochemistry and barrier heights.[40,41] However, these functionals also fail to give an initial transition state for the $CH_2O^{\bullet-} + CH_3Cl$ system. The energy release at MPW1PW91 agrees well with G3, while BMK overestimates it by about 15 kcal/mol. The initial transition state for the $CH_2O^{\bullet-} + CH_3Cl$ reaction is an S_N2-like transition state, and difficulties with density functional calculations of S_N2 reactions have been noted previously.[44,45]

Bond additivity corrections (BACs) have been used to improve the calculation of thermochemistry.[46−50] Even though this is very efficient for getting more accurate reaction enthalpies, it appears not to have been used previously in molecular dynamics calculations. Early forms of bond additivity corrections used only constants,[48] but subsequent work showed that better performance could be obtained with bond additivity corrections that are a function of the bond length.[46,47,49,50] The latter form is also suitable for correcting the potential for ab initio molecular dynamics simulations. For the reaction between formaldehyde radical anion and methyl chloride, the most important corrections are for C−C and C−Cl bond stretching potentials. The BAC functions that we have used to calculate the corrections for the $CH_2O^{\bullet-} + CH_3Cl$ potential energy surface are the following:

$$\Delta E = A_{C-C} \exp\{-\alpha_{C-C} R_{C-C}\} + A_{C-Cl} \exp\{-\alpha_{C-Cl} R_{C-Cl}\} \quad (1)$$

The parameters $A_{C-C} = 0.46$, $\alpha_{C-C} = 1.13$, $A_{C-Cl} = -0.14$, and $\alpha_{C-Cl} = 0.39$ are obtained by fitting the UHF/6-31G(d) energetics to the G3 level of theory. The corresponding corrections for the derivatives are the following:

$$\Delta \mathbf{G} = \partial(\Delta E)/\partial \mathbf{x} \quad (2)$$

$$= -\alpha_{C-C} A_{C-C} \exp\{-\alpha_{C-C} R_{C-C}\}\, \partial R_{C-C}/\partial \mathbf{x} - \alpha_{C-Cl} A_{C-Cl} \exp\{-\alpha_{C-Cl} R_{C-Cl}\}\, \partial R_{C-Cl}/\partial \mathbf{x}$$

$$\Delta \mathbf{H} = \partial^2(\Delta E)/\partial \mathbf{x}^2 \quad (3)$$

$$= \alpha_{C-C}{}^2 A_{C-C} \exp\{-\alpha_{C-C} R_{C-C}\}(\partial R_{C-C}/\partial \mathbf{x})^2 + \alpha_{C-Cl}{}^2 A_{C-Cl} \exp\{-\alpha_{C-Cl} R_{C-Cl}\}(\partial R_{C-Cl}/\partial \mathbf{x})^2$$

As can be seen from Table 1, the BAC-UHF relative energies are in reasonably good agreement with the G3 results. The BAC-UHF energy release from the TS to Sub(C) is in better agreement with the G3 results than the BH&HLYP calculations.

TABLE 3: Number of Sub(C) and Sub(C) → ET, Direct ET, Sub(O) → ET, Sub(O), and Nonreactive (NR) Trajectories

	method		
channel	UHF/ 6-31G(d)	BH&HLYP/ 6-31G(d)	BAC-UHF/ 6-31G(d)
Sub(C)	86	99	114
Sub(C) → ET	108	49	72
direct ET	2	31	14
Sub(O)	1	3	0
Sub(O) → ET	0	0	0
NR	6	21	3

It is apparent that bond additivity correction is an effective and inexpensive method for improving the quality of potential energy surfaces.

Molecular Dynamics. The foregoing discussion has identified BH&HLYP/6-31G(d) and BAC-UHF/6-31G(d) as levels of theory that may be suitable and practical for simulating the molecular dynamics of the $CH_2O^{\bullet-} + CH_3Cl$ reaction. Approximately 200 trajectories were integrated for each level of theory, starting at the transition state with initial conditions sampled from a thermal ensemble at 298 K. The results are collected in Table 3 and Figure 2 and are compared with our earlier ab initio classical trajectory study at the UHF/6-31G(d) level of theory.[15] The results can be grouped into six channels: (a) trajectories that go to Sub(C) products, (b) trajectories that first go to the Sub(C) valley but then dissociate to ET products within 600 fs, (c) trajectories that go directly to ET products, (d) trajectories that go to Sub(O) products, (e) trajectories that first go to Sub(O) products but then dissociate to ET products, and (e) trajectories that do not react (NR) but go back to reactants. For all three of the theoretical methods, the Sub(C) and Sub(C) → ET numbers show that most of the trajectories initially go into the Sub(C) valley but a substantial fraction of these dissociate to ET products. A much smaller number go directly to ET products. Very few go to Sub(O) products, and none of these were seen to dissociate to ET products. Even though the initial velocities along the transition vector were directed to products, some trajectories returned to reactants without reacting. Although the three levels of theory show broad similarities, there are important differences in the ratios of trajectories in these channels.

Of the total number of trajectories that go into the Sub(C) valley (i.e., Sub(C) + Sub(C) → ET), the UHF calculations yield the largest fraction (56%) dissociating to ET products and the BH&HLYP calculations the smallest fraction (33%). The UHF calculations have the largest energy release from the transition state to Sub(C) products and hence have the most energy available to surmount the barrier to the ET valley. The somewhat higher Sub(C) → ET barrier at BH&HLYP than at BAC-UHF may account for the slightly lower fraction of Sub(C) → ET

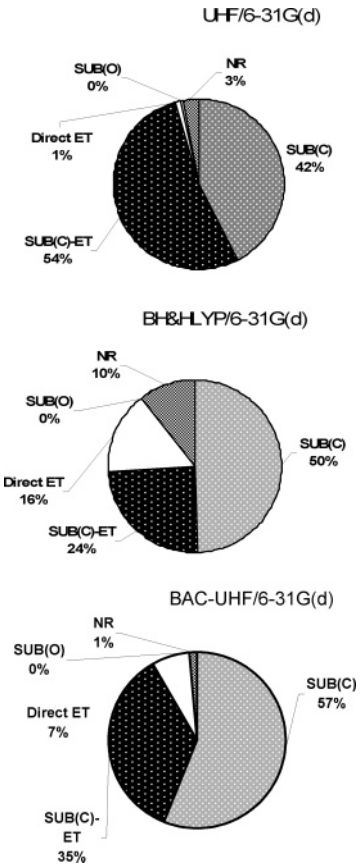

Figure 2. Branching ratios at the UHF/6-31G(d), BH&HLYP/6-31G(d), and BAC-UHF/6-31G(d) levels of theory and at 298 K.

trajectories for the former (33% vs 39%). The BH&HLYP calculations show the largest number of direct ET trajectories. This is in accord with previous findings that longer C−C distances in the transition state correlate with more electron transfer reactivity.[10,51] The BH&HLYP level of theory also yields a large number of nonreactive trajectories. The early transition state coupled with a relatively flat potential energy surface in the transition state region may increase the probability that a trajectory is reflected back to the reactants.

The reaction of $CH_2O^{\bullet-}$ with CH_3Cl deposits a substantial amount of energy in the newly formed C−C bond. This leads to chemically activated dissociation of the C−C bond in the Sub(C) → ET channel. Figure 3 plots the logarithm of the number of undissociated $CH_3CH_2O^{\bullet}$ molecules in the Sub(C) → ET channel. The nearly linear plots are indicative of first-order kinetics as expected for a unimolecular dissociation. For the UHF and BAC-UHF cases, about half of these trajectories have dissociated by 190−200 fs. However, ∼250 fs is required for half of the BH&HLYP trajectories to dissociate. This is primarily due to the earliness of the BH&HLYP transition state. As a result, the BH&HLYP trajectories take 40−60 fs longer than the UHF and BAC-UHF trajectories to reach the region of the potential energy surface where dissociation can begin. The rate constants for dissociation determined for the three levels of theory are remarkably similar, -0.024 ± 0.002, -0.021 ± 0.002, and -0.019 ± 0.001 fs^{-1} for UHF, BH&HLYP, and BAC-UHF, respectively.

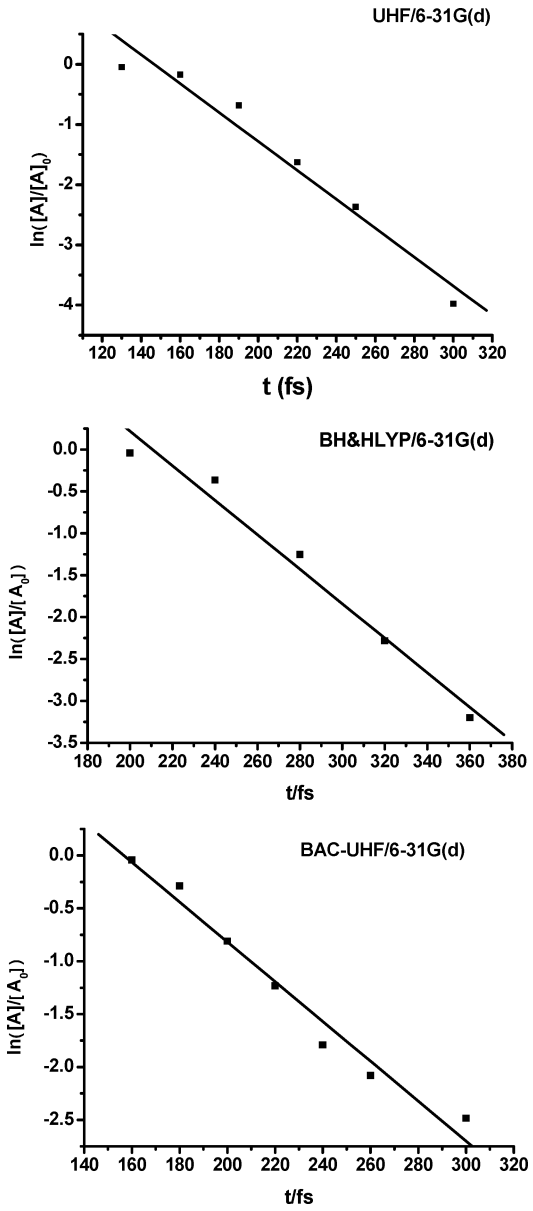

Figure 3. Plot showing the first-order kinetics for Sub(C) → ET dissociation at the UHF/6-31G(d), BH&HLYP/6-31G(d), and BAC-UHF/6-31G(d) levels of theory and at 298 K.

Summary

Ab initio classical trajectory calculations were used to study the branching ratios for the reaction between formaldehyde radical anion and methyl chloride. Calculations with the G3 and CBS-QB3 methods showed that earlier studies at the Hartree−Fock level of theory overestimated the energy release from the transition state by up to a factor of 3. The energetics at a variety of less costly levels of theory were compared to the more accurate G3 values to find a balance between accuracy and affordability for ab initio dynamics calculations. DFT calculations were affordable and offered improved energetics compared to Hartree−Fock, but most functionals failed to yield an optimized transition state for this reaction. The exceptions were the BH&H and BH&HLYP functionals, but these produced transitions states that are too early along the reaction path. A bond additivity correction (BAC) scheme was constructed to improve the Hartree−Fock potential energy surface by fitting functions to the G3 energetics. Ab initio classical trajectories were calculated with the BH&HLYP/6-31G(d) and BAC-UHF/6-31G(d) methods and were compared to earlier calculations at the UHF/6-31G(d) level of theory. Because the transition state is too early with the DFT methods, the BH&HLYP molecular dynamics calculations overestimated the number of nonreactive and direct ET trajectories. In the UHF/6-31G(d) calculations,

more than half of the trajectories that initially went into the Sub(C) valley dissociated to ET products. For the BH&HLYP and BAC-UHF calculations, only about one-third of the Sub-(C) trajectories dissociate to ET products. Both of these methods yield a better value for the calculated energy release from the initial transition state and an improved Sub(C) → ET barrier height when compare to the G3 results. The present calculations suggest that bond additivity corrections provide a practical and widely applicable method for improving potential energy surfaces for ab initio trajectory calculations. In combination with inexpensive methods such as Hartree−Fock and calibrated against accurate methods such as G3, bond additivity corrections can yield better molecular dynamics results without significantly increasing the computational cost.

Acknowledgment. This work was supported by a grant from the National Science Foundation (CHE 0512144). The authors thank Dr. Xiaosong Li for helpful discussion and Wayne State University C&IT and ISC for computer time.

References and Notes

(1) Ingold, C. *Structure and mechanism in organic chemistry*, 2nd ed.; Cornell University Press: Ithaca, NY, 1969; pp ix, 1266.

(2) Lowry, T. H.; Richardson, K. S. *Mechanism and theory in organic chemistry*, 3rd ed.; Harper & Row: New York, 1987; pp xii, 1090.

(3) Bakken, V.; Danovich, D.; Shaik, S.; Schlegel, H. B. *J. Am. Chem. Soc.* **2001**, *123*, 130−134.

(4) Bertran, J.; Gallardo, I.; Moreno, M.; Saveant, J. M. *J. Am. Chem. Soc.* **1996**, *118*, 5737−5744.

(5) Kimura, N.; Takamuku, S. *Bull. Chem. Soc. Jpn.* **1991**, *64*, 2433−2437.

(6) Kimura, N.; Takamuku, S. *J. Am. Chem. Soc.* **1994**, *116*, 4087−4088.

(7) Sastry, G. N.; Danovich, D.; Shaik, S. *Angew. Chem., Int. Ed. Engl.* **1996**, *35*, 1098−1100.

(8) Sastry, G. N.; Shaik, S. *J. Am. Chem. Soc.* **1995**, *117*, 3290−3291.

(9) Sastry, G. N.; Shaik, S. *J. Phys. Chem.* **1996**, *100*, 12241−12252.

(10) Sastry, G. N.; Shaik, S. *J. Am. Chem. Soc.* **1998**, *120*, 2131−2145.

(11) Shaik, S.; Danovich, D.; Sastry, G. N.; Ayala, P. Y.; Schlegel, H. B. *J. Am. Chem. Soc.* **1997**, *119*, 9237−9245.

(12) Yamataka, H.; Aida, M.; Dupuis, M. *Chem. Phys. Lett.* **1999**, *300*, 583−587.

(13) Yamataka, H.; Aida, M.; Dupuis, M. *Chem. Phys. Lett.* **2002**, *353*, 310−316.

(14) Yamataka, H.; Aida, M.; Dupuis, M. *J. Phys. Org. Chem.* **2003**, *16*, 475−483.

(15) Li, J.; Li, X. S.; Shaik, S.; Schlegel, H. B. *J. Phys. Chem. A* **2004**, *108*, 8526−8532.

(16) Garst, J. F. *Acc. Chem. Res.* **1971**, *4*, 400−406.

(17) Garst, J. F.; Smith, C. D. *J. Am. Chem. Soc.* **1976**, *98*, 1520−1526.

(18) Screttas, C. G.; Michascrettas, M. *J. Phys. Chem.* **1983**, *87*, 3844−3847.

(19) Lund, H.; Daasbjerg, K.; Lund, T.; Pedersen, S. U. *Acc. Chem. Res.* **1995**, *28*, 313−319.

(20) Lund, T.; Lund, H. *Tetrahedron Lett* **1986**, *27*, 95−98.

(21) Lund, T.; Lund, H. *Acta Chem. Scand. B* **1988**, *42*, 269−279.

(22) Eberson, L. *New J. Chem.* **1992**, *16*, 151−156.

(23) Curtiss, L. A.; Raghavachari, K.; Redfern, P. C.; Rassolov, V.; Pople, J. A. *J. Chem. Phys.* **1998**, *109*, 7764−7776.

(24) Montgomery, J. A.; Frisch, M. J.; Ochterski, J. W.; Petersson, G. A. *J. Chem. Phys.* **1999**, *110*, 2822−2827.

(25) Montgomery, J. A.; Frisch, M. J.; Ochterski, J. W.; Petersson, G. A. *J. Chem. Phys.* **2000**, *112*, 6532−6542.

(26) Frisch, M. J.; Trucks, G. W.; Schlegel, H. B.; Scuseria, G. E.; Robb, M. A.; Cheeseman, J. R.; Montgomery, J. A.; Vreven, T.; Kudin, K. N.; Burant, J. C.; Millam, J. M.; Iyengar, S.; Tomasi, J.; Barone, V.; Mennucci, B.; Cossi, M.; Scalmani, G.; Rega, N.; Petersson, G. A.; Nakatsuji, H.; Hada, M.; Ehara, M.; Toyota, K.; Fukuda, R.; Hasegawa, J.; Ishida, M.; Nakajima, T.; Honda, Y.; Kitao, O.; Nakai, H.; Klene, M.; Li, X.; Knox, J. E.; Hratchian, H. P.; Cross, J. B.; Adamo, C.; Jaramillo, J.; Gomperts, R.; Stratmann, R. E.; Yazyev, O.; Austin, A. J.; Cammi, R.; Pomelli, C.; Ochterski, J.; Ayala, P. Y.; Morokuma, K.; Voth, G. A.; Salvador, P.; Dannenberg, J. J.; Zakrzewski, V. G.; Dapprich, S.; Daniels, A. D.; Strain, M. C.; Farkas; Malick, D. K.; Rabuck, A. D.; Raghavachari, K.; Foresman, J. B.; Ortiz, J. V.; Cui, Q.; Baboul, A. G.; Clifford, S.; Cioslowski, J.; Stefanov, B. B.; Liu, G.; Liashenko, A.; Piskorz, P.; Komaromi, I.; Martin, R. L.; Fox, D. J.; Keith, T.; Al-Laham, M. A.; Peng, C. Y.; Nanayakkara, A.; Challacombe, M.; Gill, P. M. W.; Johnson, B.; Chen, W.; Wong, M. W.; Andres, J. L.; Gonzalez, C.; Replogle, E. S.; Pople, J. A. *Gaussian 03, Development Version*, revision D.02.

(27) Bolton, K.; Hase, W. L.; Schlegel, H. B.; Song, K. *Chem. Phys. Lett.* **1998**, *288*, 621−627.

(28) Millam, J. M.; Bakken, V.; Chen, W.; Hase, W. L.; Schlegel, H. B. *J. Chem. Phys.* **1999**, *111*, 3800−3805.

(29) Bakken, V.; Millam, J. M.; Schlegel, H. B. *J. Chem. Phys.* **1999**, *111*, 8773−8777.

(30) Hase, W. L. Classical Trajectory Simulations: Initial Conditions. In *Encyclopedia of Computational Chemistry*; Schleyer, P. v. R., Allinger, N. L., Clark, T., Gasteiger, J., Kollman, P. A., Scheafer, H. F., III, Schreiner, P. R.; Wiley: Chichester, U.K., 1998; pp 402−407.

(31) Peslherbe, G. H.; Wang, H. B.; Hase, W. L. *Adv. Chem. Phys.* **1999**, *105*, 171−201.

(32) Becke, A. D. *J. Chem. Phys.* **1993**, *98*, 5648−5652.

(33) Becke, A. D. *J. Chem. Phys.* **1996**, *104*, 1040−1046.

(34) Perdew, J. P.; Burke, K.; Wang, Y. *Phys. Rev. B* **1996**, *54*, 16533−16539.

(35) Perdew, J. P.; Chevary, J. A.; Vosko, S. H.; Jackson, K. A.; Pederson, M. R.; Singh, D. J.; Fiolhais, C. *Phys. Rev. B* **1992**, *46*, 6671−6687.

(36) Perdew, J. P.; Chevary, J. A.; Vosko, S. H.; Jackson, K. A.; Pederson, M. R.; Singh, D. J.; Fiolhais, C. *Phys. Rev. B* **1993**, *48*, 4978−4978.

(37) Becke, A. D. *Phys. Rev. A* **1988**, *38*, 3098−3100.

(38) Lee, C.; Yang, W.; Parr, R. D. *Phys. Rev. B* **1988**, *37*, 785−789.

(39) Miehlich, B.; Savin, A.; Stoll, H.; Preuss, H., *Chem. Phys. Lett.* **1989**, *157*, 200−206.

(40) Adamo, C.; Barone, V. *J. Chem. Phys.* **1998**, *108*, 664−675.

(41) Boese, A. D.; Martin, J. M. L. *J. Chem. Phys.* **2004**, *121*, 3405−3416.

(42) Durant, J. L. *Chem. Phys. Lett.* **1996**, *256*, 595−602.

(43) Baker, J.; Andzelm, J.; Muir, M.; Taylor, P. R. *Chem. Phys. Lett.* **1995**, *237*, 53−60.

(44) Glukhovtsev, M. N.; Bach, R. D.; Pross, A.; Radom, L. *Chem. Phys. Lett.* **1996**, *260*, 558−564.

(45) Deng, L. Q.; Branchadell, V.; Ziegler, T. *J. Am. Chem. Soc.* **1994**, *116*, 10645−10656.

(46) Allendorf, M. D.; Melius, C. F. *J. Phys. Chem. A* **2005**, *109*, 4939−4949.

(47) Anantharaman, B.; Melius, C. F. *J. Phys. Chem. A* **2005**, *109*, 1734−1747.

(48) Ho, P.; Coltrin, M. E.; Binkley, J. S.; Melius, C. F. *J. Phys. Chem.* **1985**, *89*, 4647−4654.

(49) Ho, P.; Melius, C. F. *J. Phys. Chem.* **1990**, *94*, 5120−5127.

(50) Melius, C. F.; Allendorf, M. D. *J. Phys. Chem. A* **2000**, *104*, 2168−2177.

(51) Shaik, S.; Shurki, A. *Angew. Chem., Int. Ed. Engl.* **1999**, *38*, 586−625.